Photoluminescence of Tensile Strained, Exactly Strain Compensated, and Compressively Strained $Si_{1-x-y}Ge_xC_y$ Layers on Si

O. G. Schmidt and K. Eberl

Max-Planck-Institut für Festkörperforschung, Heisenbergstraße 1, 70569 Stuttgart, Germany

(Received 19 November 1997)

Band edge related photoluminescence is observed from strain compensated $Si_{1-x-y}Ge_xC_y$ multiple quantum wells. For (87 ± 4) Å thick quantum wells, the no-phonon energy decreases linearly with increasing C content as $-y$(6.8 eV). The band gap for unstrained $Si_{1-y}C_y$ material is deduced for carbon concentrations lower than 0.85%. An initial energy increase and a subsequent energy decrease on the way from tensile strained $Si_{1-y}C_y$ and from compressively strained $Si_{1-x}Ge_x$ alloys towards exactly strain compensated $Si_{1-x-y}Ge_xC_y$ structures is measured. The different band alignments and strain-induced electron and hole level crossing effects are discussed. [S0031-9007(98)05791-3]

PACS numbers: 78.66.Li, 73.20.Dx, 78.55.Hx, 81.10.–h

Adding carbon into the SiGe material system substantially extends the design freedom for SiGe-based heterostructures: First, the smaller carbon atom can compensate compressive strain in $Si_{1-x}Ge_x$ layers on Si [1] and thus relieves thickness limitations in strained-layer growth. Second, the major band offset in $Si_{1-y}C_y$ quantum wells (QWs) is found in the conduction band [2], which, in connection with the valence band offset in $Si/Si_{1-x}Ge_x$ heterostructures, has already opened up a wide variety of new electronic and optical properties within the SiGe material system. However, although the band gaps of pseudomorphic $Si_{1-x}Ge_x$ and $Si_{1-y}C_y$ (up to a C concentration of 2%) have been experimentally determined [2,3], there has been little work dealing with the regime between these two alloys. In fact, to our knowledge, no data have been published about the band gap of *exactly strain compensated* $Si_{1-x-y}Ge_xC_y$ QWs, nor have there been any reports on the band gap of *tensile strained* $Si_{1-x-y}Ge_xC_y$ layers. This Letter focuses on the band edge related photoluminescence (PL) of tensile strained and exactly strain compensated $Si_{1-x-y}Ge_xC_y$ layers and thus provides a more complete picture of the band gap and band alignment for the binary $Si/Si_{1-y}C_y$, $Si/Si_{1-x}Ge_x$, and ternery $Si/Si_{1-x-y}Ge_xC_y$ heterostructures.

All samples are grown by molecular beam epitaxy. Details on the growth procedures and the PL setup are given elsewhere [2]. The structural properties of the samples are determined by x-ray diffraction (XRD) and by comparing the data with dynamical simulation results, which are based on Vegard's law and linearly interpolated elastic constants between Si and diamond. Experimental data for the exact lattice constants $a_0(y)$ and elastic constants of unstrained $Si_{1-y}C_y$ alloys are not available at present. Kelires [4] has calculated $a_0(y)$ and found a slight bowing effect between Si and diamond. Using the theoretical data from Kelires reduces the carbon concentrations indicated in the following by about 30%, but it does not change the other statements.

Figure 1(a) presents x-ray diffraction rocking curves of 30-period (87 ± 4) Å $Si_{1-x-y}Ge_xC_y$/(108 ± 5) Å Si superlattices. The dominating peak, observed in all three curves, originates from the Si substrate. In the upper spectrum the carbon fraction is zero and compressive strain is introduced by 3.7 ± 0.1% Ge. The lateral compression of the $Si_{0.963}Ge_{0.037}$ layer results in a vertical lattice extension due to the Poisson ratio. As a result the zeroth order superlattice peak (0-SL) is shifted to negative angles compared to the Si substrate peak. The bottom curve is obtained from a $Si_{1-y}C_y/Si$ superlattice with $y = (0.45 \pm 0.02)\%$. Since the carbon atom is much smaller than the Si atom, tensile strain is introduced, and the 0-SL peak is shifted to positive angles. Note that this shift, apart from its opposite direction, is exactly the same as for the $Si_{1-x}Ge_x/Si$ superlattice. For the sample shown in the middle of Fig. 1(a) the C and Ge fractions are added together. As expected, the 0-SL peak exactly coincides with the Si-substrate peak and only the first-order superlattice peaks (−1-SL and 1-SL) can be resolved. Hence, from a structural point of view

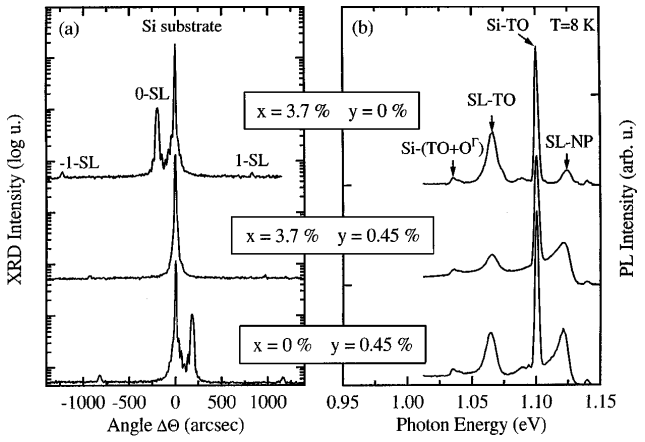

FIG. 1. XRD rocking curves and PL spectra of three 30-period (87 ± 4) Å $Si_{1-x-y}Ge_xC_y$/(108 ± 5) Å Si superlattices. For the strain compensated $Si_{1-x-y}Ge_xC_y$ structure in the middle row of (a) the 0-SL diffraction peak exactly coincides with the Si substrate peak. The corresponding PL spectrum in (b) shows superlattice related no-phonon and TO-phonon replica peaks directly proving a smaller band gap of strain compensated $Si_{1-x-y}Ge_xC_y$ compared to Si.

 0031-9007/98/80(15)/3396(4)$15.00

strain compensated $Si_{1-x-y}Ge_xC_y$ exhibits Si-like lattice symmetry neglecting local strain effects within the alloy. Figure 1(b) shows PL spectra taken from the same three superlattices. The Si-TO and the Si-(TO + O^{Γ}) lines at energies $E = 1.099$ and 1.035 eV originate from the Si substrate, buffer, and cap layers. The spectra reveal two additional PL lines which are attributed to the no-phonon (NP) line and the Si-Si TO-phonon replica of excitons confined in the $Si_{1-x-y}Ge_xC_y$ layers. It is remarkable that the strain compensated sample also shows these two PL lines, which directly demonstrates a reduced band gap in strain compensated $Si_{1-x-y}Ge_xC_y$ layers compared to pure Si. Since the strain is completely compensated we attribute this band gap reduction to purely intrinsic effects of Ge and C. Although this was proposed in earlier works [5,6], it is the first time that this effect has been directly measured.

Figure 2 shows the energetic peak position of the NP lines of a series of exactly strain compensated $Si_{1-x-y}Ge_xC_y$ multiple quantum well (MQW) samples with varied x and y. Exact strain compensation in these samples was checked by XRD measurements yielding similar rocking curves to that presented in the middle of Fig. 1(a). The superlattice related NP lines shift linearly down in energy with increasing C and Ge content. The experimental data are fitted by a linear decrease in PL energy of about $\Delta E = -x(0.84\ \text{eV})$, or equivalently of about $\Delta E = -y(6.80\ \text{eV})$. Inserted error bars take into account energy uncertainties due to determination of well widths and alloy compositions. The fitted straight line extrapolates to an energy of 1.151 eV. A small energy offset of 4 meV compared to the free exciton in Si can be explained by excitons bound to local QW width or alloy fluctuations [2]. Figure 2 also shows the well-known free-exciton energy of unstrained $Si_{1-x}Ge_x$ bulk material as a function of Ge content [3]. If we assume that intrinsic band gap reductions ΔE_{SiC} and ΔE_{SiGe} due to C and Ge, respectively, add up linearly to ΔE_{SiGeC} for strain compensated $Si_{1-x-y}Ge_xC_y$ QWs, then we can determine the band gap reduction ΔE_{SiC} of unstrained $Si_{1-y}C_y$ bulk material by

$$\Delta E_{\text{SiC}} = \Delta E_{\text{SiGeC}} - \Delta E_{\text{SiGe}} = -y(2.7\ \text{eV}), \quad y \le 0.85\%. \tag{1}$$

A cross-check on the validity of this assumption is obtained by subtracting the calculated tensile strain effect $\Delta E_{\text{SiC, strain}}$ from the measured band gap reduction of a pseudomorphic $Si_{1-y}C_y$ layer $\Delta E_{\text{SiC, pseu}}$:

$$\Delta E_{\text{SiC}} = \Delta E_{\text{SiC, pseu}} - \Delta E_{\text{SiC, strain}}. \tag{2}$$

From the PL measurements on $Si_{1-y}C_y$ samples we deduce $\Delta E_{\text{SiC, pseu}} = -y(6.6\ \text{eV})$ which almost exactly agrees with the extrapolated band gap reduction from Ref. [2]. Using Si deformation potential parameters we obtain $\Delta E_{\text{SiC, strain}} = -y(4.6\ \text{eV})$. This includes the strain-induced down-shift of the ($\Delta 2$) minima in the conduction band and the energy shift of the light holes in the valence band. Inserting these values into Eq. (2) yields $\Delta E_{\text{SiC}} = -y(2.0\ \text{eV})$, which is slightly smaller than the value obtained from Eq. (1). However, for 1% C the difference amounts to 7 meV which is in the range of uncertainties in the deformation potentials.

In the following, we investigate the near-band edge PL behavior in the regime between strained $Si_{1-x}Ge_x$ and $Si_{1-y}C_y$ layers. Figure 3(a) contains previously published PL data of $Si_{1-y}C_y$ and $Si_{1-x-y}Ge_xC_y$ layers. The dashed lines represent the band gap of compressively (negative) strained $Si_{1-x}Ge_x$ and tensile (positive) strained $Si_{1-y}C_y$ structures. We note that experimental PL data exist only for compressively strained $Si_{1-x-y}Ge_xC_y$ structures, while in the tensile strain regime investigations are limited to binary $Si_{1-y}C_y$ layers [2]. Figure 3(b) enlarges and focuses on the upper section of Fig. 3(a). The dotted line in the negative strain regime represents the band gap of unstrained $Si_{1-x}Ge_x$ bulk material. Our new experimental data are shown as solid squares and dots. For the $Si_{1-x}Ge_x$ QWs the NP energies are slightly higher than the corresponding fundamental band gap. Because of the small effective mass of the heavy holes (hh) [3], confinement in the (87 ± 4) Å thick QWs still blueshifts the hh energy level by about 10 meV. The transverse electron mass in the $Si_{1-y}C_y$ layers is much larger ($0.92m_e$), and the confinement effect is expected to shift energies by only 1–3 meV [2]. Thus, the experimental PL data are very close to the band gap line for tensile strained $Si_{1-y}C_y$. The three solid squares at the top are taken from the PL spectra presented in Fig. 1(b). We concentrate the following discussion on the lower curve, starting at a strain value of $\varepsilon = -0.003\,13$. If we reduce the compressive strain in the $Si_{0.93}Ge_{0.07}$ by introducing substitutional C and at the same time leaving the Ge concentration constant, the no-phonon energy shifts to higher energy. This agrees with previously reported PL data depicted in Fig. 3(a) [5–7]. Further increase of the C content towards full strain compensation in Si/SiGeC, however, results in a reduction of

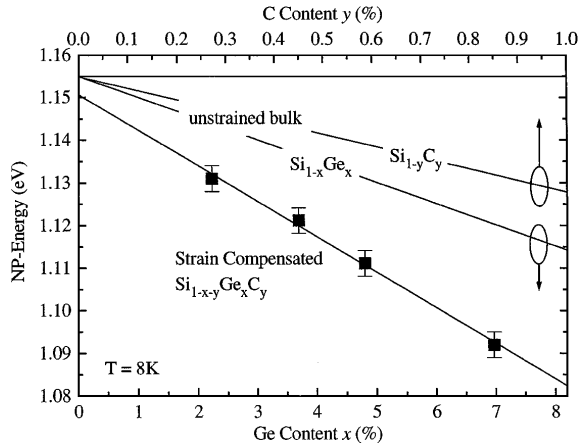

FIG. 2. NP energy as a function of C and Ge fraction for exactly strain compensated $Si_{1-x-y}Ge_xC_y$, unstrained $Si_{1-x}Ge_x$, and unstrained $Si_{1-y}C_y$ bulk alloys. $Si_{1-x}Ge_x$ and $Si_{1-y}C_y$ curves extrapolate to the free-exciton energy in Si at 8 K. A slight offset of 4 meV for $Si_{1-x-y}Ge_xC_y$ might be due to bound exciton luminescence.

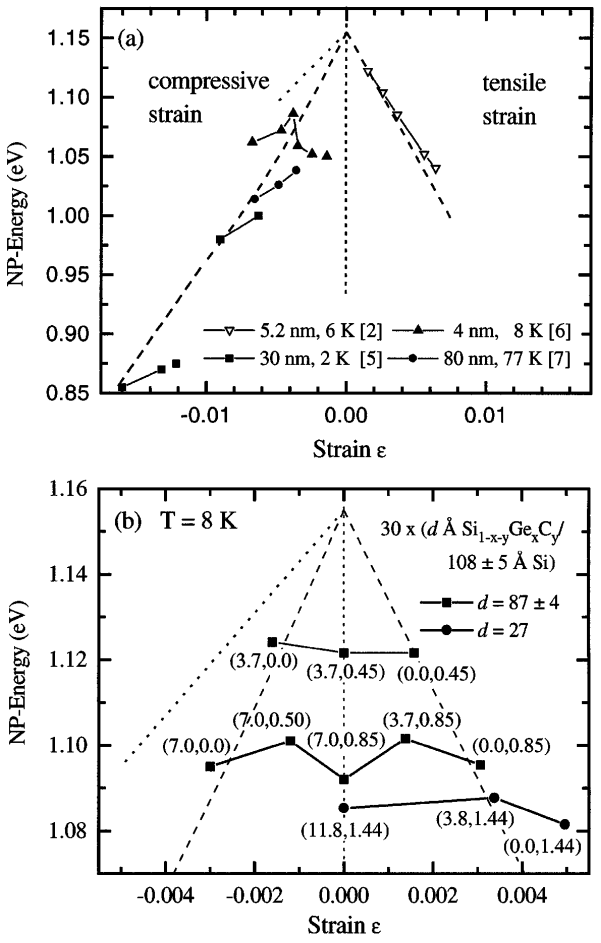

FIG. 3. NP energy as a function of strain. In (a) PL data of recent work are summarized. QW thicknesses and temperatures are indicated in the legend; (b) shows an enlarged section of the upper part of (a) with PL data in the compressive (negative) strain regime and in the tensile (positive) strain regime. Dashed lines represent fundamental band gaps of binary alloys. The dotted line is the band gap of unstrained $Si_{1-x}Ge_x$. Numbers in brackets represent x and y fractions in % of $Si_{1-x-y}Ge_xC_y$ quantum wells.

the no-phonon PL energy. We already reported this behavior for narrow $Si_{0.84-y}Ge_{0.16}C_y$ QWs with higher Ge content as shown in Fig. 3(a) (full triangles) [6]. Similar behavior is observed in the positive strain regime starting at a tensile strain value $\varepsilon = +0.003\,13$ for pseudomorphic $Si_{0.9915}C_{0.0085}$ QWs. Adding a certain amount of Ge reduces tensile strain and the NP energy is initially blueshifted. However, for the exactly strain compensated $Si_{0.9215}Ge_{0.07}C_{0.0085}$ layer an energy decrease compared to both the positive and the negative strain regimes is observed. The initial blueshift and the redshift beyond a certain Ge content x are confirmed for $Si/Si_{0.9856-x}Ge_xC_{0.0144}$ QWs shown as full dots in the lower right part of Fig. 3(b). The PL energy of the $Si_{0.9856}C_{0.0144}$ sample, which is the right dot at $\varepsilon = 0.005$, is considerably above the dashed line. This is due to the significant confinement shift in the 27 Å narrow QW.

Figure 4 shows a schematic diagram of the band-edge alignment of the three distinct alloy combinations within the $Si/Si_{1-x-y}Ge_xC_y$ material system, namely, compressively strained $Si_{1-x}Ge_x$, strain compensated $Si_{1-x-y}Ge_xC_y$, and tensile strained $Si_{1-y}C_y$. The band alignment of pseudomorphic $Si/Si_{1-x}Ge_x$ was recently clearly identified by low excitation PL as type II [8] with the main band offset in the valence band (VB) and only a very small offset of about 10 meV in the conduction band (CB) as schematically illustrated on the left side of Fig. 4. We verified this result by an excitation dependent PL measurement for the 87 Å $Si_{0.93}Ge_{0.07}$ QWs, where we observe a 5 meV energy shift of the NP peak due to band bending. The excitation power density was varied from 2.5 mW cm^{-2} to 2.5 W cm^{-2} in this experiment. Compressive in-plane strain in SiGe lifts degeneracy and splits the VB into heavy hole (hh) and light hole (lh) states with the hh defining the VB maxima [3]. Likewise, the sixfold degenerate CB is split into ($\Delta 2$) and ($\Delta 4$) valleys with the ($\Delta 4$) states being the CB minimum. In contrast to that, $Si/Si_{1-y}C_y$ heterostructures are type I [2] with about 70% of the band offset in the CB [9]. For the tensile strained 27 Å $Si_{0.9856}C_{0.0144}$ structure we measure only a minor 1–2 meV energy shift of the NP-PL line with increasing excitation density confirming a type-I band alignment. Again, the CB and VB are split by biaxial strain into ($\Delta 2$) and ($\Delta 4$) as well as into heavy and light hole states, respectively. In contrast to SiGe, now the ($\Delta 2$) states form the CB minima and the lh states are the VB maxima as shown in the right part of Fig. 4. In a perfectly strain compensated $Si/Si_{1-x-y}Ge_xC_y$ heterostructure, lh and hh VB and ($\Delta 2$) and ($\Delta 4$) CB states regain degeneracy just like in Si, neglecting carrier confinement effects. For the strain compensated 27 Å $Si_{0.8676}Ge_{0.118}C_{0.0144}$ structure an excitation dependent energy shift of 3.3 meV is measured.

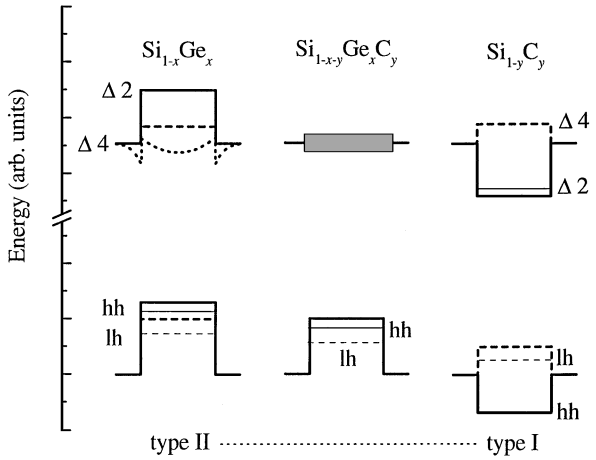

FIG. 4. Schematic band-edge diagram of the three distinct structures within the $Si_{1-x-y}Ge_xC_y$ alloy system, namely, $Si_{1-x}Ge_x$, $Si_{1-y}C_y$, and strain compensated $Si_{1-x-y}Ge_xC_y$. Confinement energy levels are indicated as thinner lines. Since the transition type for $Si_{1-x-y}Ge_xC_y$ is not known, the uncertainty is shown as the grey-shaded area in the CB. The dotted line in the CB of the $Si/Si_{1-x}Ge_x$ QW indicates charged carrier induced band bending which creates triangular potentials at the interfaces.

This and a simple interpolation between $Si/Si_{1-y}C_y$ and $Si/Si_{1-x}Ge_x$ implies an optical transition with a rather small band offset in the CB. However, the exact band offset is not known yet, and this uncertainty is marked by the grey-shaded area in Fig. 4. Since our $Si/Si_{1-x-y}Ge_xC_y$ heterostructures consist of QWs with 87 Å thickness, the confinement effect must be considered. For $Si/Si_{1-x}Ge_x$ light holes and heavy holes are shifted to lower energies as indicated by thinner dashed and full lines on the left side of Fig. 4. In the type-II CB band bending due to space charges [8] must be considered especially in conditions of high excitation power. This creates triangular potentials at the $Si/Si_{1-x}Ge_x$ interfaces as schematically indicated by the dotted line in Fig. 4 for the CB, where ($\Delta 4$) and ($\Delta 2$) states become localized. The confinement level of localized ($\Delta 4$) states will be shifted to lower energies than the ($\Delta 2$) states, since the ($\Delta 4$) potential barrier is much smaller than the band offset for ($\Delta 2$).

For type-I $Si/Si_{1-y}C_y$ QWs the confinement effect shifts the lh states in the VB away from the band edge to lower energies as well as the ($\Delta 2$) states in the CB to higher energies. The confinement levels are again indicated by thinner full and dashed lines for the ($\Delta 2$) and the lh states in Fig. 4, respectively. Although the band edges in the CB and the VB are degenerate for strain compensated $Si/Si_{1-x-y}Ge_xC_y$ charge carrier confinement introduces a splitting of the energy states due to the different effective masses. In the VB the heavier hh states will form the maximum energy level. In the CB the heavier transverse effective mass of the ($\Delta 2$) states shifts the confinement energy below the ($\Delta 4$) level. This is also the case for type-II band alignment due to charge carrier induced band bending effects at the interfaces especially at high excitation power in PL.

From the above discussion we deduce that on the way from $Si/Si_{1-x}Ge_x$ to strain compensated $Si/Si_{1-x-y}Ge_xC_y$ heterostructures the hh states stay energetically higher than the lh, whereas in the CB ($\Delta 2$) and ($\Delta 4$) states undergo an energy level crossing due to the confinement effects. In the tensile strain regime the situation is reversed: ($\Delta 2$) states stay lowest in energy while lh and hh states in the VB exhibit an energy level crossing. These two energy crossings qualitatively explain the "energy dip" observed in Fig. 3(b). Additionally, a transition from type II for $Si/Si_{1-x}Ge_x$ and type I for $Si/Si_{1-y}C_y$ can add to the energy lowering measured for strain compensated $Si/Si_{1-x-y}Ge_xC_y$. A more quantitative description will be published elsewhere [10].

A further contribution to the no-phonon PL-energy lowering for strain compensated $Si/Si_{1-x-y}Ge_xC_y$ may be due to local strain inhomogeneities within the layer. It turns out that planar epitaxial growth of fully strain compensated $Si_{1-x-y}Ge_xC_y$ with x larger than 15% (that means C content above 2%) becomes more and more difficult, whereas strained $Si/Si_{1-x}Ge_x$ and $Si/Si_{1-y}C_y$ with equivalent Ge and C concentrations still show high crystal quality. That means lattice matched $Si_{1-x-y}Ge_xC_y$ layers with Ge and C concentrations significantly above the samples discussed in this paper are difficult to grow thicker than about 10 nm on Si without significant surface roughening caused by local strain around substitutional C atoms. Obviously, bonds between C and Ge are unfavorable to form but become increasingly more difficult to avoid for higher Ge concentrations. The local atomic structure of strain compensated $Si_{1-x-y}Ge_xC_y$ alloys on Si has been discussed in detail by Dietrich *et al.* [11]. Local strain fields introduced by substitutional C broaden the Si-Si, Si-Ge, and the Ge-Ge phonon peaks by elongating bonds close to the C atoms. The Raman results indicate that the Si-Si bonds are not identical to those in unstrained bulk Si for strain compensated $Si_{1-x-y}Ge_xC_y$ alloys which have the same average lattice constant [11]. Lorentzen *et al.* [12] discussed the possibility of band gap lowering in SiGeC due to C-induced localized energy levels. Further experiments, especially for samples with higher C concentrations, will be required to determine the exact contributions in band gap shift due to band structure changes, on the one hand, and localized energy levels, on the other hand.

In conclusion, we have for the first time observed near-band-edge PL of exactly strain compensated $Si_{1-x-y}Ge_xC_y$ alloy layers. For (87 ± 4) Å thick QWs the no-phonon PL energy decreases linearly as $-x(0.86\ \text{eV})$ or equivalently as $-y(6.8\ \text{eV})$. From this we deduce a linear energy reduction for unstrained $Si_{1-y}C_y$ of $-y(2.7\ \text{eV})$ with increasing C content. An initial PL-energy increase on the way from tensile strained $Si_{1-y}C_y$ as well as from compressively strained $Si_{1-x}Ge_x$ alloys towards exactly strain compensated $Si_{1-x-y}Ge_xC_y$ structures is observed. An energy lowering for strain compensated $Si_{1-x-y}Ge_xC_y$ structures is observed and can be explained by energy level crossings due to confinement effects.

The authors thank K. von Klitzing for his continuous interest and support. The very skillful support of W. Winter is extremely valuable.

[1] K. Eberl *et al.*, Appl. Phys. Lett. **60**, 3033 (1992).
[2] K. Brunner, K. Eberl, and W. Winter, Phys. Rev. Lett. **76**, 303 (1996).
[3] For a review, see *Properties of Strained and Relaxed Silicon Germanium,* edited by E. Kasper, emis Data Review Series Vol. 12 (INSPEC, London, 1995).
[4] P. C. Kelires, Phys. Rev. Lett. **75**, 1114 (1995); Phys. Rev. B **55**, 8784 (1997).
[5] A. St. Amour *et al.*, Appl. Phys. Lett. **67**, 3915 (1995).
[6] K. Eberl, K. Brunner, and W. Winter, Thin Solid Films **294**, 98 (1997).
[7] P. Boucaud *et al.*, Appl. Phys. Lett. **64**, 875 (1994).
[8] M. L. W. Thewalt *et al.*, Phys. Rev. Lett. **79**, 269 (1997).
[9] R. L. Williams *et al.*, Appl. Phys. Lett. **72**, 1320 (1998).
[10] R. Hartmann *et al.* (to be published).
[11] B. Dietrich *et al.*, Phys. Rev. B **49**, 17 185 (1994).
[12] J. D. Lorentzen *et al.*, Appl. Phys. Lett. **70**, 2353 (1997).